Nanoscale

COMMUNICATION

View Article Online
View Journal | View Issue

Cite this: *Nanoscale*, 2014, **6**, 11066

Received 2nd April 2014
Accepted 1st August 2014

DOI: 10.1039/c4nr01780c

www.rsc.org/nanoscale

Graphene oxide assisted spontaneous growth of V_2O_5 nanowires at room temperature†

Minoh Lee,‡[a] Won G. Hong,‡[b] Hu Young Jeong,[c] Suresh Kannan Balasingam,[d] Zonghoon Lee,[c] Sung-Jin Chang,[e] Byung Hoon Kim*[f] and Yongseok Jun*[g]

Graphene-decorated single crystalline V_2O_5 nanowires (G–VONs) have been synthesized by mixing graphene oxide (GO) and V_2O_5 suspensions at room temperature. In this process, V_2O_5 nanowires (VONs) are formed spontaneously from commercial V_2O_5 particles with the aid of GO. The as-formed one dimensional G–VONs were characterized by using a X-ray diffractometer, a X-ray photoelectron spectrometer, a scanning electron microscope, and a transmission electron microscope. GO plays a vital role in the VON formation with the simultaneous reduction of GO. A single G–VON showed superior electrical conductivity compared with that of the pure VONs obtained from the sol–gel method. This could be ascribed to the insertion of rGO sheets into the V_2O_5 layered structure, which was further confirmed by electron energy loss spectroscopy.

Introduction

In recent years, the nanostructured vanadium oxides and their derivatives have been considered promising materials, and extensive research on these materials has been carried out due to their tremendous physical and chemical properties.[1] Among the various vanadium oxide nanostructures, vanadium pentoxide nanowires (VONs) have attracted much interest for their potential applications in actuators,[2] electrochromic devices,[3] Li-ion batteries,[4] and supercapacitors[5] based on their unique one dimensional (1D) structure, high surface area, and versatile redox active behavior.[6–8] Although VONs have a relatively higher surface area and in turn improved Li-ion diffusion rate in energy storage devices, their moderate electrical conductivity has been a major restriction to practical applications of this material.[9] For that reason, extensive studies have been carried out to improve the electrical conductivity of VONs by modification with carbonaceous nanomaterials.[10–12] Carbon modification facilitates an increase in electrical conductivity and also prevents vanadium dissolution, which could enhance the cycling durability of Li-ion batteries.[13,14] The research trend with the carbon modification of other materials often involves the use of graphene due to its excellent physical and chemical properties.[15–18] Unfortunately, synthesis of pristine graphene sheets requires highly controlled vacuum deposition techniques such as CVD and thermal decomposition, and the mass production of single crystalline graphene sheets is very difficult with existing techniques.[19] Hence, researchers have been focused on the bulk synthesis of graphene oxide from naturally abundant graphite *via* vigorous chemical oxidation actions.[20] In contrast to pristine graphene sheets, graphene oxide sheets have been synthesized on a large-scale by the functionalization of their basal planes and sheet edges with hydroxyl, epoxide, carbonyl and carboxyl groups.[21] These functional groups can be reduced either with high temperature treatment or by the strong reducing agents, and convert GO into rGO, which is analogous to the graphene sheets.[22] Recently, VONs and graphene hybrid nanocomposites have been synthesized by numerous approaches. For example, Liu *et al.* prepared graphene–VONs composites *via* a hydrothermal method using commercial V_2O_5 particles (VO), graphite, and the oxidizing agent, H_2O_2. They explained that VONs were formed on two dimensional graphene under hydrothermal conditions, and further, graphene sheets were formed due to the vigorous reaction of H_2O_2 and $[VO4]^-$ ions on the raw graphite

[a]*Department of Chemical Engineering, Ulsan National Institute of Science and Technology (UNIST), Ulsan 689-798, Republic of Korea*
[b]*Division of Materials Science, Korea Basic Science Institute, Daejeon 305-333, Republic of Korea*
[c]*School of Materials Science and Engineering, Ulsan National Institute of Science and Technology (UNIST), Ulsan 689-798, Republic of Korea*
[d]*Department of Chemistry, Ulsan National Institute of Science and Technology (UNIST), Ulsan 689-798, Republic of Korea*
[e]*Department of Chemistry, Chung-Ang University, Seoul 156-756, Republic of Korea*
[f]*Department of Physics, Incheon National University, Incheon 406-772, Republic of Korea. E-mail: kbh37@incheon.ac.kr; Tel: +82-032-835-8229*
[g]*Department of Materials Chemistry & Engineering, Konkuk University, Seoul 143-701, Republic of Korea. E-mail: yjun@konkuk.ac.kr; Tel: +82-02-450-0440*

† Electronic supplementary information (ESI) available: See DOI: 10.1039/c4nr01780c

‡ These authors contributed equally to this work

powder.[6,23–27] Du *et al.* also synthesized graphene–VONs composites by simple mixing of VONs and reduced GO (rGO), followed by filtration. The corresponding VONs were separately prepared by the hydrothermal method and GO was converted into rGO by the reducing agent, $NaBH_4$.[28] Recently, Perera *et al.* synthesized a hybrid graphene–VONs composite through the dropwise addition of vanadium(v) oxytriisopropoxide on rGO sheets which were then heated in an autoclave for 24 h[29] However, the graphene–VONs mixtures synthesized by the above mentioned methods need either some vigorous oxidizing agents or extraordinary conditions like high temperature and pressure. Interestingly, studies on GO have expanded to discover that GO can be used as an oxidant to oxidize a variety of organic compounds such as alcohols, alkenes, and hydrating alkynes, to their corresponding oxidized forms such as ketone, aldehyde, *etc.*[30,31]

Fig. 1 Schematic representation of G–VONs synthesis. (a) Without GO dispersion V_2O_5 nanostructures were not formed, but (b). With the addition of GO dispersions G–VONs are formed spontaneously in 7–8 weeks.

In this communication, for the first time we have reported a facile approach for the synthesis of graphene–decorated VONs (G–VONs) without any extra chemicals or external energy. 1D G–VONs have been fabricated by simple mixing of GO and VO in deionized water at room temperature. In this process GO acts as an oxidant. Since the oxidizing agent generally becomes reduced, GO was converted into rGO. More interestingly, the electrical conductivity of a single G–VON was found to be higher than that of pure VONs obtained from the sol–gel method.

Results and discussions

Fig. 1 shows the schematic representation of the experimental plan. While under the controlled experimental conditions (room temperature and D.I water), there is no change in morphology of VO particles observed even after 6 months (Fig. 1(a)), however, G–VONs have formed in 7–8 weeks after simple mixing of VO and GO suspension (Fig. 1(b)). Different pH values produced by adding nitric acid or sulfuric acid did not change the morphology of VO from the condition shown in Fig. 1(a) in months. SEM images of pristine VO particles and GO are shown in Fig. 2(a) and (b). The structure of VO particles in DI water did not change even after 6 months, as mentioned above (Fig. 2(c)). After mixing the VO and GO suspensions, GO sheets have begun wrapping VO in the first week as shown in Fig. 2(d). As time goes on, nanowires are gradually formed, as observed 5 weeks later (Fig. 2(e)). After 7–8 weeks, the mixture has completely turned into G–VONs (Fig. 2(f)). The structure of the G–VONs was investigated by X-ray diffraction (XRD) and selected area electron diffraction (SAED) (Fig. 3). The XRD pattern of VO (black line) shows the crystalline orthorhombic phase, which is in good agreement with the standard pattern

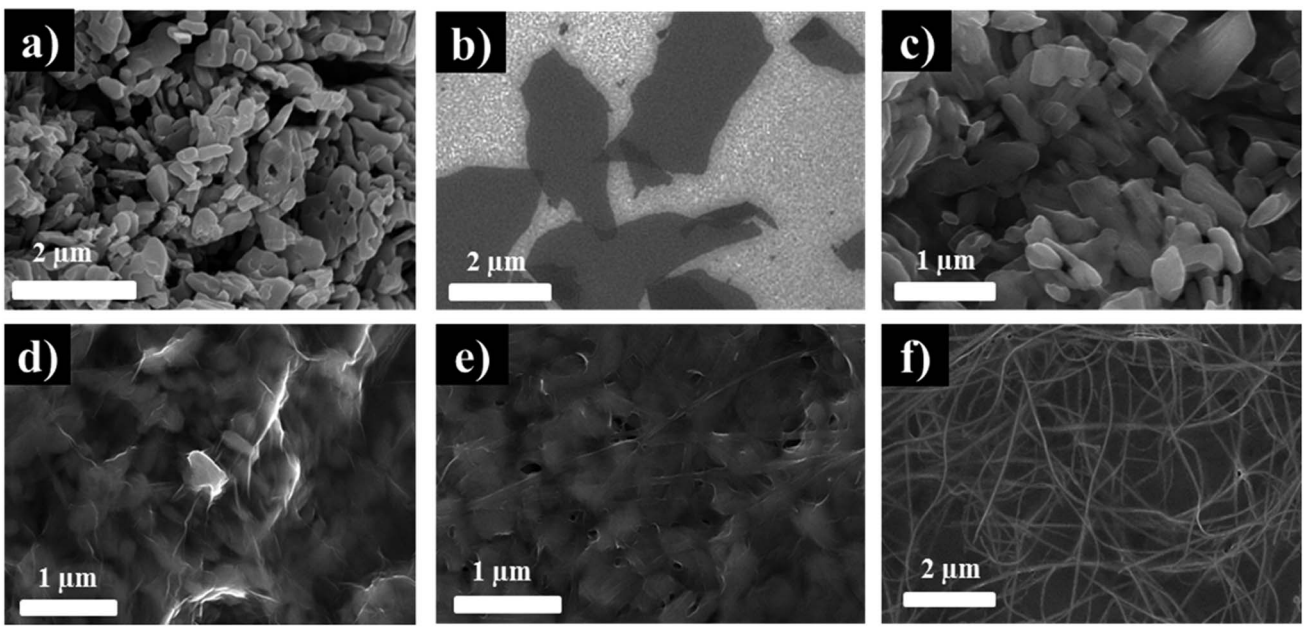

Fig. 2 SEM images of (a) VO, (b) as synthesized GO, and (c) VO after 6 months without GO suspension. The mixture of GO and VO (d) after 1 week, (e) after 5 weeks, and (f) after 8 weeks.

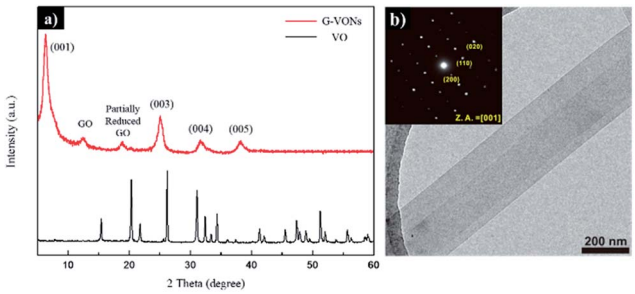

Fig. 3 Structure of G–VONs. (a) XRD spectra of G–VONs (red line) and VO (black line) measured in the 2θ range of 5° to 60° (b) SAED of single G–VON.

(JCPDS Card no. 89-0612). The XRD pattern of G–VONs (red line) contains GO-related peaks as well as the VONs peaks. The peaks at $2\theta = 6.26°$, 25°, 31.64° and 38.2° are respectively assigned to the orthorhombic phase of VONs with the corresponding lattice planes of (001), (003), (004) and (005). The peak at 12.36° and 18.84° corresponds to the (002) plane of GO and partially reduced GO, respectively.[8,32] The XRD study shows the layered structure of G–VONs. From the (001) reflection, the interlayer distance of the G–VONs is determined to be 1.41 nm, which is larger than the reported value (1.15 nm) for the pure VONs.[3,33] Fig. 3(b) shows the SAED pattern of 300 nm wide G–VONs. The indexing confirmed the orthorhombic crystalline V_2O_5 phase (lattice parameters, $a = 12.1$ Å, $b = 3.81$ Å, $c = 14.1$ Å) with a preferential nanowire growth direction along the [010] direction. Compared to the pure VONs (a = 11.722 Å, $b = 3.570$ Å, $c = 11.520$ Å),[8] the G–VONs have a distorted crystal structure, and the corresponding lattice parameters are larger than for the pure VONs. Both analyses support the conclusion that the interlayer distance has increased by 3 Å at maximum, and this may be ascribed to the insertion of rGO sheets into the V_2O_5 crystal structure. In addition, we also conducted a spatially resolved Raman spectroscopy to prove the existence of the rGO in the G–VONs. As shown in Fig. 4, the graphitic D peak (a) and G peak (b) are clearly drawn in a given space. The bright parts with orange color (maximum intensity with 37.1×10^3) could represent (r)GO flakes on the surface. Another bright region with pale blue gives a nanowire shape is also depicted by graphitic D/G peaks, and this indicates that rGO is evenly distributed in VONs. Elemental analyses are confirmed by scanning transmission electron microscopy (STEM) and electron energy loss spectroscopy (EELS) analyses were performed (Fig. 5). It was clearly observed that the G–VONs grew from the original V_2O_5 seed as shown in High-angle annular dark field (HAADF) STEM images (Fig. 5(a) and (b)). It is worth pointing out that the GO points 1 and 2 represented by red dots were G–VONs and GO, respectively. EELS of both points proved it. The EELS C–K and V–L edges are shown in G–VONs (Fig. 5(d)) but EELS C–K and O–K edges developed in GO (Fig. 5(e)). Interestingly, the intensity of the O–K edge is quite low compared with the C–K edge, indicating the reduction of GO, which will be discussed later. Three elements were also identified with EELS element mapping. Fig. 5(f)–(i) show the HAADF STEM image, and EELS mapping for the elements vanadium, oxygen, and carbon, respectively. Although the quantity of carbon element is small, it demonstrates that VO is decorated with rGO sheets. The carbon peak did not reduce even after strong plasma etching in a chamber which normally removes adsorbed carbon on the surface. Fig. S1, ESI† shows the C 1s and V 2p peaks for G–VONs. The oxygen functional groups were prominently reduced after 8 weeks without any external factors (hydrothermal, heat treatment *etc.*) or reducing reagent. The peaks observed at 515.8 eV and 517.5 eV correspond to the +4 and +5 oxidation states of vanadium compound, respectively.

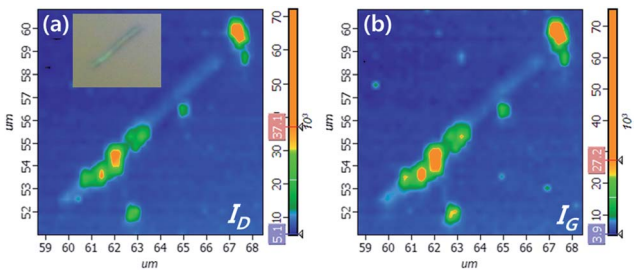

Fig. 4 Intensities of (a) D and (b) G band obtained by spatially resolved Raman spectroscopy of single G–VON. The inset of (a) shows the optical image of the G–VONs.

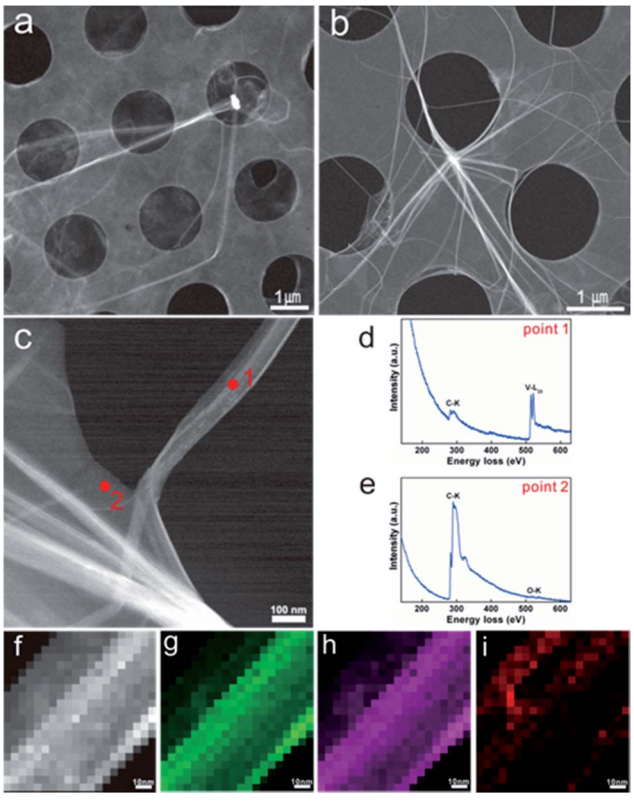

Fig. 5 HAADF STEM images of G–VONs. (a and b) The nanowires are grown from V_2O_5 seeds. (c) STEM image for EELS study. EELS spectra at the region of the red spot 1 (d) and spot 2 (e). (f) HAADF STEM image of G–VONs and the corresponding EELS element mapping (g) Vanadium, (h) oxygen, and (i) Carbon.

VO showed the V^{4+}/V^{5+} ratio of 0.096. When the VO suspension was mixed with the GO dispersion, the ratio of V^{4+}/V^{5+} decreased to 0.055 within 1 day. This means that most of the vanadium 4+ valence states were oxidized to +5 states by the GO sheets. From this observation, we concluded that GO played the role of the oxidizing agent. Therefore, the mechanism of VON formation could be predicted as follows. First, when VO meets GO in D.I. water medium, the abundant functional groups present on the GO sheets, such as hydroxyl, carboxyl and carbonyl, might attach on the surface of VO through chemical bonds.[34] Then, GO sheets become widely spread on the surface of VO and oxidation is initiated by the oxygen containing functional groups *via* transfer of electrons between VO and GO during the oxidation process. V_2O_5 mixing with the +4 valence state of the vanadium atom may be oxidized to the soluble form, seed, and regrow as the V_2O_5 nanostructure on the surface of graphene in the direction of the (001) plane.[24] The dimensional nanowire grows continuously in length and width with time until it is saturated. Meanwhile, the oxygen functional groups of GO decrease, resulting in the increase of the portion of the C–C bond from 37.4 to 67.3% in the G–VONs mixture (see Fig. S1†). Temperature-dependent electrical transport properties of a single VON (separated from the G–VONs mixture) are shown in Fig. 6. To compare the resistance values of VONs and G–VONs, we have first measured the current-voltage (*I–V*) characteristics of VONs synthesized by a sol–gel method. However, there was no noticeable current observed for a VON made *via* the sol–gel method. In the case of G–VONs, we observed a reasonable current at room temperature; the measured current was around 1.6 nA at 3.0 V even for a single G–VON. This higher conductivity of the single wire V_2O_5 (separated from the G–VONs mixture) may be due to the insertion of rGO into the V_2O_5 layers as shown in the TEM, XPS, and spatially resolved Raman spectroscopy results. Highly symmetric *I–V* characteristics (Fig. 6(a) and (b)) were observed over the whole temperature range (105–417 K) and the non-linear behavior was enhanced at the low temperature range (Fig. 6(b)). The resistance ($R(T)$) obtained from the linear region near 0.0 V increases with a decrease in temperature, which indicates an insulating behavior (Fig. 6(c)). A small polaronic conduction has been generally accepted as the main transport mechanism of VONs.[7] However, a variable range hopping (VRH) conduction (inset of Fig. 6(c)) is better fitted to the $R(T)$ rather than the small polaronic conduction. Since the VRH conduction occurs when the electronic states are localized and randomly distributed in non-crystalline materials,[35] we suggest that rGO cause disorder in VONs. This is well consistent with the TEM and XRD results. *I–V* characteristics of a single G–VON and VONs were also compared in Fig. S3.† Since the reasonable current could not be obtained in a single VON, we measured lots of VONs between electrodes 1 and 2 as shown in Fig. S3 (b).† Even though there were many VONs between the electrodes, the current was smaller than that of a single G–VON at an applied bias voltage of 3 V (0.83 nA for VONs and 1.6 nA for G–VONs). Finally, the synthesized G–VONs were applied as a cathode material for Li-ion batteries. Due to the high conductivity of G–VONs, the specific capacity and rate capability of G–VONs are superior to that of pure VONs (see Fig. S4 in the ESI†). This indicates that G–VONs could be a potential candidate for energy storage devices such as rechargeable Li-ion batteries.

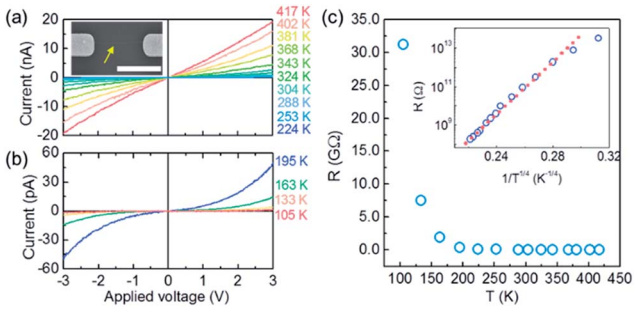

Fig. 6 Electrical transport property of single G–VON. (a and b) Temperature-dependent *I–V* characteristics. The inset shows the SEM image of the measured sample. The scale bar is 2 μm. (c) Temperature-dependent resistance shows an insulating behavior. Three dimensional VRH can explain the conduction mechanism of single G–VON (inset).

Experimental

Preparation of graphene oxide (GO)

GO was prepared by the modified Hummer's method.[36] About 10 g of $K_2S_2O_8$ and 10 g of P_2O_5 were dissolved in 50 mL of concentrated H_2SO_4 at 80 °C, followed by the addition of 12 g of graphite powder. This mixture was diluted with 2 L of deionized (DI) water and left overnight. After that the mixture was filtered, washed, and then dried to obtain the pre-oxidized graphite oxide. The product was re-suspended in a concentrated sulfuric acid. And then $KMnO_4$ was gradually added into the suspension with simultaneous stirring at 0 °C. Around 3.7 L of DI water and 50 mL of 30 wt% H_2O_2 were added until the bubbles disappeared. The GO suspension was centrifuged with 5 L of 10% HCl solution, followed by washing with 5 L of DI water. In order to remove any residual metal ions, the product was dialyzed for 2 weeks. And finally, GO was obtained by drying this aqueous dispersion at 40 °C for 3 days in an oven.

Synthesis of graphene–decorated V_2O_5 nanowires (G–VONs)

Commercially available V_2O_5 particles (Aldrich, 0.03 g) and the as synthesized GO (0.01 g) were separately mixed into 10 mL of DI water. Then, the dispersed GO solution was added into the V_2O_5 dispersion followed by constant stirring of the mixture for 3 h at room temperature. The mixture was kept at room temperature without further stirring. G–VONs grew spontaneously with the simultaneous reduction of GO over time. The time taken for the complete growth of G–VONs was at least 8 weeks. For comparison, the vanadium pentoxide suspension was also prepared by the same procedure without adding the GO dispersion.

Characterization

The surface morphology of the resulting products was observed using field-emission scanning electron microscopy (FE-SEM, Nano230, FEI co.) at 10 kV. The crystal structures of the

as-synthesized materials were characterized using X-ray diffraction analysis (XRD, Bruker D8 Advance with Cu Kα radiation, $\lambda = 1.54178$ Å). Spatially resolved Raman spectra of the samples were measured using a NT-MDT NTEGRA system, in which a Raman spectrometer is combined with a scanning probe microscope. To measure Raman spectroscopy, the G–VON suspension was dropped onto 300 nm of SiO_2 substrate. The Raman spectra were recorded using a laser excitation of 472.7 nm, whose spot size is limited by diffraction. The measurements were performed at room temperature, which is stably maintained by the air-conditioning system, using a 100× objective with a very incident power of 23 μW to avoid sample damage or laser inducing heating. X-ray photoelectron spectroscopy (XPS, Thermo Fisher, UK) was employed with monochromatic Al Kα radiation as the X-ray source. Bright-Field (BF) TEM, electron diffraction pattern, and electron energy loss spectroscopy (EELS) were carried out with an image-side aberration-corrected TEM (Titan3 G2 60-300, FEI) which operated at 80 kV. High-angle annular dark field (HAADF) scanning transmission electron microscopy (STEM) was performed using a probe-side aberration-corrected TEM (JEOL 2100F, JEOL) operated at 200 kV.

Electrical transport property measurement

To measure electrical transport properties, G–VONs were deposited onto 300 nm SiO_2/highly p-doped Si wafers. Electrodes were fabricated by conventional electron beam lithography (acceleration voltage: 30 keV). Ti/Au (5/50 nm) were deposited using an e-gun evaporation system in high vacuum ($<5 \times 10^{-6}$ Torr) and lift-off procedures. Temperature-dependent *I–V* characteristics were measured by the conventional two-probe method in the Janis cryogenic system with a semiconductor characterization system (4200-SCS, Keithley). The electrical measurements were performed under vacuum conditions ($<2 \times 10^{-3}$ Torr).

Conclusions

We have reported the spontaneous formation of graphene–decorated V_2O_5 nanowires (G–VONs) *via* a facile room temperature process. This approach is considered to be eco-friendly due to the absence of any hazardous chemicals or energy input. The spontaneously formed G–VONs were found to have a good electricity property compared with that of the pure V_2O_5 nanowires (VONs). The higher conductivity was attributed to the insertion of rGO sheets into the layered crystal structure of VONs. Our approach may open the door to fabricate 1D nanostructures of different metal oxides using GO as an aiding agent. Although the rGO sheets position in 1D-VONs is not clear at this moment, the insertion of rGO sheets has improved the electrical properties of VONs.

Acknowledgements

This work was supported by the New & Renewable Energy Core Technology Program of the KETEP (No. 20133030000140) and Ministry of Science, ICT and Future Planning (No. 2013059244). B. H. Kim acknowledges support from National Research Foundation of Korea (NRF-2014R1A1A1002467).

Notes and references

1 Y. Wang and G. Cao, *Chem. Mater.*, 2006, **18**, 2787–2804.
2 G. Gu, M. Schmid, P. W. Chiu, A. Minett, J. Fraysse, G. T. Kim, S. Roth, M. Kozlov, E. Muñoz and R. H. Baughman, *Nat. Mater.*, 2003, **2**, 316–319.
3 C. Xiong, A. E. Aliev, B. Gnade and K. J. Balkus,Jr, *ACS Nano*, 2008, **2**, 293–301.
4 Y. Wang, K. Takahashi, K. Lee and G. Cao, *Adv. Funct. Mater.*, 2006, **16**, 1133–1144.
5 G. Wee, H. Z. Soh, Y. L. Cheah, S. G. Mhaisalkar and M. Srinivasan, *J. Mater. Chem.*, 2010, **20**, 6720–6725.
6 J. Livage, *Chem. Mater.*, 1991, **3**, 578–593.
7 J. Muster, G. T. Kim, V. Krstić, J. G. Park, Y. W. Park, S. Roth and M. Burghard, *Adv. Mater.*, 2000, **12**, 420–424.
8 V. Petkov, P. N. Trikalitis, E. S. Bozin, S. J. L. Billinge, T. Vogt and M. G. Kanatzidis, *J. Am. Chem. Soc.*, 2002, **124**, 10157–10162.
9 A. Singhal, G. Skandan, G. Amatucci, F. Badway, N. Ye, A. Manthiram, H. Ye and J. J. Xu, *J. Power Sources*, 2004, **129**, 38–44.
10 Z. Chen, V. Augustyn, J. Wen, Y. Zhang, M. Shen, B. Dunn and Y. Lu, *Adv. Mater.*, 2011, **23**, 791–795.
11 S. D. Perera, B. Patel, N. Nijem, K. Roodenko, O. Seitz, J. P. Ferraris, Y. J. Chabal and K. J. Balkus Jr, *Adv. Energy Mater.*, 2011, **1**, 936–945.
12 J. W. Lee, S. Y. Lim, H. M. Jeong, T. H. Hwang, J. K. Kang and J. W. Choi, *Energy Environ. Sci.*, 2012, **5**, 9889–9894.
13 M. Koltypin, V. Pol, A. Gedanken and D. Aurbach, *J. Electrochem. Soc.*, 2007, **154**, A605–A613.
14 A. Pan, D. Liu, X. Zhou, B. B. Garcia, S. Liang, J. Liu and G. Cao, *J. Power Sources*, 2010, **195**, 3893–3899.
15 A. K. Geim and K. S. Novoselov, *Nat. Mater.*, 2007, **6**, 183–191.
16 U. N. Maiti, W. J. Lee, J. M. Lee, Y. Oh, J. Y. Kim, J. E. Kim, J. Shim, T. H. Han and S. O. Kim, *Adv. Mater.*, 2014, **26**, 40–67.
17 W. J. Lee, T. H. Hwang, J. O. Hwang, H. W. Kim, J. Lim, H. Y. Jeong, J. Shim, T. H. Han, J. Y. Kim, J. W. Choi and S. O. Kim, *Energy Environ. Sci.*, 2014, **7**, 621–626.
18 T. H. Han, W. J. Lee, D. H. Lee, J. E. Kim, E. Y. Choi and S. O. Kim, *Adv. Mater.*, 2010, **22**, 2060–2064.
19 C. N. R. Rao, A. K. Sood, K. S. Subrahmanyam and A. Govindaraj, *Angew. Chem., Int. Ed.*, 2009, **48**, 7752–7777.
20 O. C. Compton and S. T. Nguyen, *Small*, 2010, **6**, 711–723.
21 S. Stankovich, D. A. Dikin, G. H. B. Dommett, K. M. Kohlhaas, E. J. Zimney, E. A. Stach, R. D. Piner, S. T. Nguyen and R. S. Ruoff, *Nature*, 2006, **442**, 282–286.
22 S. Pei and H. M. Cheng, *Carbon*, 2012, **50**, 3210–3228.
23 X. Ren, Y. Jiang, P. Zhang, J. Liu and Q. Zhang, *J. Sol-Gel Sci. Technol.*, 2009, **51**, 133–138.
24 H. Liu and W. Yang, *Energy Environ. Sci.*, 2011, **4**, 4000–4008.
25 F. Zhou, X. Zhao, C. Yuan, L. Li and H. Xu, *Chem. Lett.*, 2007, **36**, 310–311.

26 F. Zhou, X. Zhao, Y. Liu, C. Yuan and L. Li, *Eur. J. Inorg. Chem.*, 2008, 2506–2509.
27 M. Li, F. Kong, H. Wang and G. Li, *CrystEngComm*, 2011, **13**, 5317–5320.
28 G. Du, K. H. Seng, Z. Guo, J. Liu, W. Li, D. Jia, C. Cook, Z. Liu and H. Liu, *RSC Adv.*, 2011, **1**, 690–697.
29 S. D. Perera, A. D. Liyanage, N. Nijem, J. P. Ferraris, Y. J. Chabal and K. J. Balkus,Jr, *J. Power Sources*, 2013, **230**, 130–137.
30 D. R. Dreyer, S. Park, C. W. Bielawski and R. S. Ruoff, *Chem. Soc. Rev.*, 2010, **39**, 228–240.
31 H. P. Jia, D. R. Dreyer and C. W. Bielawski, *Tetrahedron*, 2011, **67**, 4431–4434.
32 B. H. Kim, W. G. Hong, H. R. Moon, S. M. Lee, J. M. Kim, S. Kang, Y. Jun and H. J. Kim, *Int. J. Hydrogen Energy*, 2012, **37**, 14217–14222.
33 B. H. Kim, H. Y. Yu, W. G. Hong, J. Park, S. C. Jung, Y. Nam, H. Y. Jeong, Y. W. Park, Y. Jun and H. J. Kim, *Chem.–Asian J.*, 2012, **7**, 684–687.
34 W. G. Hong, B. H. Kim, S. M. Lee, H. Y. Yu, Y. J. Yun, Y. Jun, J. B. Lee and H. J. Kim, *Int. J. Hydrogen Energy*, 2012, **37**, 7594–7599.
35 E. A. Davis and N. F. Mott, *Philos. Mag.*, 1970, **22**, 903–922.
36 V. C. Tung, M. J. Allen, Y. Yang and R. B. Kaner, *Nat. Nanotechnol.*, 2009, **4**, 25–29.